

ICSV14

Cairns • Australia
9-12 July, 2007



THREE-DIMENSIONAL PREDICTIONS OF THE ROD WAKE-AIRFOIL INTERACTION NOISE BY HYBRID METHODS

Björn Greschner^{1*}, Sven Peth¹, Young J. Moon², Jung H. Seo², Marc C. Jacob³, Frank Thiele¹

¹Berlin University of Technology
Institute of Fluid Mechanics and Engineering Acoustic
Mueller-Breslau-Str. 8
D-10623 Berlin, Germany

²Korea University
Department of Mechanical Engineering
1 Anam-dong, Sungbuk-ku
Seoul, 136-701, Korea

³Ecole Centrale de Lyon
Centre Acoustique du LMFA-UMR CNRS 5509
36, avenue Guy de Collogne
F-69134 Ecully, France
greschner@cf.d.tu-berlin.de

Abstract

Sound generated by an airfoil in the wake of a rod is predicted numerically by two different hybrid CFD/CAA approaches ($Ma = 0.2$). The configuration is a symmetric airfoil one chord downstream of a rod, whose wake contains both periodic and broadband vortical fluctuations. In particular, a significant broadening of the main Strouhal peak has been observed at subcritical vortex shedding conditions. This study addresses the overall ability of both CFD/CAA hybrid approaches to model broadband noise sources. The first approach computes the aerodynamic noise by solving the linearized perturbed compressible equations (LPCE) for the noise propagation, with the acoustic sources and hydrodynamic flow variables computed from the incompressible Large Eddy Simulation (iLES) using a computational grid of approximately 3 million grid cells and high-order compact finite difference schemes. The second approach uses the unsteady aerodynamic field of a compressible Detached Eddy Simulation (DES) and a Ffowcs Williams & Hawkings (FW-H) acoustic analogy formulation for the farfield noise calculations. The non-zonal DES approach solves either the unsteady Reynolds-averaged or spatially filtered Navier-Stokes equations by using a novel cubic explicit algebraic stress turbulence model based on a two-equation k-e model by Lien and Lechziner. An implicit formulation is used with second order accuracy and a grid of approximately 2.3 million cells. The results of these hybrid approaches are compared and subsequently validated with the measurements of Jacob *et al.* in the nearfield (HWA) and in the farfield (noise).

1. INTRODUCTION

Recent studies have shown that the rod-airfoil test case is particularly suitable for the assessment of CFD codes in modeling broadband noise sources. The configuration is that of a symmetric airfoil ($c = 0.1$ m) located one chord downstream of a rod ($d = 0.01$ m), whose wake contains both periodic and broadband vortical fluctuations. In particular, a significant broadening of the main Strouhal peak has been observed at subcritical vortex shedding conditions [1]. Different authors have already demonstrated the excellent capabilities of the fully resolved compressible LES to model broadband noise; thus the propagation of the noise to the farfield is the pitfall of these kind of methods, because the scales in time and space diverge. So the next logical step consists in developing methods for industrial applications that are able to reproduce and propagate the broadband noise with a reasonable computational effort. In this paper two different hybrid approaches will be discussed to cover these contrary requirements, the DES/FW-H method and the iLES/LPCE approach on the other side.

The Detached Eddy Simulation (DES) restrict the LES domain to unsteady turbulent flow regions and use simpler closures elsewhere. They are expected to approach the quality of a LES prediction with optimised computational costs. In combination with the Ffowcs-Williams and Hawkings (FW-H) integral method the predicted noise in the farfield shows reasonable results and are therefore a good candidate for this kind of applications, as shown by the authors in a previous paper [2]. A closer inspection shows that the inclusion of non-linear sound sources requires the simulation of the compressible Navier-Stokes equations in the nearfield. This causes many problems in setup and stability of the flow simulation system, especially for low mach number cases as the presented rod-wake airfoil interaction. In the presented paper this hybrid approach is named DES/FW-H. On the other hand a hydrodynamic splitting method from Seo and Moon [3] is applied to avoid the compressible flow simulation. The two parts of this new method consist of an incompressible three-dimensional Large Eddy Simulation (iLES) that computes the hydrodynamic properties and in the second step the two-dimensional acoustic field is calculated by the Linearized Perturbed Compressible Equations (LPCE) [3]. Subsequently, there is a 2D Kirchhoff extrapolation to the far-field and a 3D correction after Oberai [4]. An important advantage in the splitting is the computational efficiency. The iLES is in 3D, but the LPCE is performed as a 2D calculation. Both solvers are independent from each other, they even use different grids which are optimized for their particular needs. The objective of this study is to evaluate critically these hybrid methods by comparing the aerodynamic and aeroacoustic results with the experiment measured at EC Lyon from Jacob et al. [1]. Section 2 is devoted to the detailed description of the numerical approaches and whereas section 3 describes the flow configuration and the setup. Section 4 provides an overview of the aerodynamic results and finally section 5 is specifically concerned with the sound computations. The conclusions are drawn in section 6.

2. HYBRID METHODS

The comparison of the presented hybrid methods are a result of the collaborative research work of the Korea University (KU) and the Berlin University of Technology (TUB). This section is devoted to a short overview of the methods developed at both universities and describes shortly the differences of the used flow solvers.

2.1. DES & FW-H method

The DES/FW-H approach has been commonly used for approximately 6 years by TU Berlin. The DES is still in development to improve the quality of the simulation results. TUB uses the in house solver ELAN for research and development of new background models of the DES. In the first part of this section a brief introduction is given for ELAN. The FW-H approach is a standard method for the farfield sound calculation [5].

2.1.1. ELAN flow solver

The unsteady aerodynamic field is computed by using an in-house finite-volume code ELAN that solves either the unsteady Reynolds-averaged or spatially filtered Navier-Stokes equations employing a RANS or Large Eddy Simulation, respectively. An implicit formulation is used with second order accuracy both in space and in time. All scalar quantities, as well as the cartesian components of tensorial quantities are stored in the cell centres of arbitrarily curvilinear, semi-structured grids that can fit very complex geometries with the desired local refinement level. Linear momentum equations are solved sequentially, with the pressure field computed at each time step via a separate iterative procedure based on a pressure-correction scheme of the SIMPLE type with an additional compressible convection term as described by Ferziger & Peric [6]. The set of compressible equations is completed with an equation for the total enthalpy and the ideal gas law. A generalised Rhie & Chow interpolation is used to avoid an odd-even decoupling of pressure, velocity and Reynolds-stress components. The equation system is solved by an iterative method, the well known Stone's SIP solver and the time integration is fully implicit of second order accuracy.

2.1.2. Detached Eddy Simulation

The Detached Eddy approach based on the idea of combining RANS and LES turbulence models have become increasingly popular in recent years, since they require a reduced computational effort in comparison to genuine LES, while retaining much of the physical accuracy of the method. The basic concept of DES was published in 1997 [7] and was based on the popular Spalart-Allmaras (SA) one-equation turbulence model. The peculiarity of a DES approach consists in using a single turbulence model, which behaves like a subgrid-scale model in regions where the grid density is fine enough for a LES, and like a RANS model in regions where it is not. In order to achieve this, the length scale in the underlying turbulence model is replaced by the DES length scale:

$$L_{DES} = \min(l_{RANS}, C_{DES}\Delta), \quad \Delta = \max(\Delta x, \Delta y, \Delta z) \quad (1)$$

where C_{DES} is a model constant analogous to that of the Smagorinsky constant in LES. L_{DES} is the turbulence length scale of the background RANS model and Δ is an appropriate grid size, e.g. the cell size or the cubic root of the cell volume. Therefore L_{DES} plays the role of an implicit filter width in a LES fashion, as is directly based on the local grid size. The main goal is to achieve a RANS simulation in the vicinity of solid boundaries, and LES in regions of massive flow separation outside of the boundary layer.

The presented DES based on the the Cubic Explicit Algebraic Stress $LL k - \varepsilon$ Model (CEASM). This CEASM model is a two-layer model and is developed for complex wall bounded flows. For a two equation model, the turbulence length scale l_{RANS} is based on local turbulence

quantities k and ε and appears in more than one term of the model equations. Although the standard approach consists in substituting this in the dissipation term of the k -equation, similarly to what is done in the precursor SA-DES model, both a wall normal distance and a locally-determined length scale are used in the CEASM model. For an exhaustive representation of the model equations, tensor representation and model constants, the reader is referred to Lübcke *et al.* [8].

2.1.3. Ffowcs-Williams & Hawkings method

The aeroacoustic computations are carried out by using the rotor-noise FW-H code FoxHawk. It computes the far field sound using a forward-time algorithm by Brentner [9] based on the well-known Formulation 1A by Farassat [10], extended to penetrable integration surfaces by Di Francescantonio [11] and Brentner & Farassat [12]. It is a generalization of the code Advantia described in [13] to generic body motions. The acoustic signals are calculated along with the aerodynamic field, saving both CPU-time and storage space. A permeable control surface that surrounds all bodies in the flow as well as the most turbulent regions is used for farfield noise calculation as depicted in Figure 1(d).

2.2. iLES & LPCE method

The main idea of iLES/LPCE method proposed by KU is to split the whole computation into a hydrodynamic and an acoustic part. The hydrodynamic computation is performed by an incompressible large eddy simulation (iLES), while the acoustic computation uses the linearized perturbed compressible equations [3] (LPCE).

2.2.1. Incompressible Large Eddy Simulation

The instantaneous total flow variables are decomposed into the incompressible and perturbed compressible variables. The incompressible variables represent unsteady viscous flow, while the perturbed compressible variables describe the acoustic fluctuations and all other compressible components. The exclusion of compressibility in the Navier-Stokes equations for iLES leads to the incompressible Navier-Stokes equations. Their filtered form is written as

$$\frac{\partial \tilde{U}_j}{\partial x_j} = 0, \quad \rho_0 \frac{\partial \tilde{U}_i}{\partial t} + \rho_0 \frac{\partial}{\partial x_j} (\tilde{U}_i \tilde{U}_j) = - \frac{\partial \tilde{P}}{\partial x_i} + \mu_0 \frac{\partial}{\partial x_j} \left(\frac{\partial \tilde{U}_i}{\partial x_j} + \frac{\partial \tilde{U}_j}{\partial x_i} \right) - \rho_0 \frac{\partial}{\partial x_j} M_{ij} \quad (2)$$

where the resolved states are marked by $(\tilde{\cdot})$. There are many ways to model the sub-grid tensor M_{ij} . For the present computation, the tensor is set to zero, i.e. the subgrid scale turbulence is not modeled.

The iLES is solved by an iterative implicit fractional step method (Poisson's equation for pressure). The momentum equations are time-integrated by a four stage Runge-Kutta method and spatially discretized by a sixth-order compact finite difference [14] scheme. Then the pressure field is iteratively solved to satisfy continuity, and the velocity is updated by a correction step. Consequently, LPCE is solved in a coupled manner with iLES, by acquiring the acoustic sources (DP/Dt) from iLES solution every time step.

2.2.2. LPCE and Kirchhoff

The linearized perturbed compressible equations can be derived by applying the decomposed state equations to the Navier-Stokes equations, and subtracting the compressible Navier-Stokes equations from them. The LPCE are written in a vector form as,

$$\frac{\partial \rho'}{\partial t} + (\vec{U} \cdot \nabla) \rho' + \rho_0 (\nabla \cdot \vec{u}') = 0 \quad (3)$$

$$\frac{\partial \vec{u}'}{\partial t} + \nabla (\vec{u}' \cdot \vec{U}) + \frac{1}{\rho_0} \nabla p' = 0 \quad (4)$$

$$\frac{\partial p'}{\partial t} + (\vec{U} \cdot \nabla) p' + \gamma P (\nabla \cdot \vec{u}') + (\vec{u}' \cdot \nabla) P = -\frac{DP}{Dt}. \quad (5)$$

In the present study, the aeroacoustic field at zero spanwise wave number $k_z=0$ is obtained by solving the 2D Linearized Perturbed Compressible Equations (LPCE). The 'spanwise-averaged' acoustic source (DP/Dt) and hydrodynamic variables are obtained from the iLES solution. This 2D method with subsequent Oberai's 3D correction [4] is efficient and produces sufficient results when the turbulent flow may be assumed 'statistically homogeneous' in the spanwise direction. The LPCE is time-integrated by a four-stage Runge-Kutta method and spatially discretized by a sixth-order compact finite difference scheme. For damping numerical instabilities, a tenth-order spatial filter by Gaitonde *et al.* [15] is used.

The acoustic grid covers a circular domain with a radius of $60d$. The microphones of the experiment are at a distance of $185d$ from the center of the airfoil. The extrapolation is done by a 2D Kirchhoff method in frequency domain given by,

$$4i\hat{p}' = - \int_S \left[\frac{\partial \hat{p}'}{\partial n} H_0^{(2)}(\omega r/c_0) - \frac{\omega}{c_0} (\underline{n} \cdot \underline{r}) \hat{p}' H_0^{(2)}(\omega r/c_0) \right] dS \quad (6)$$

3. FLOW CONFIGURATION AND SETUP

3.1. Reference experiment

An experimental investigation of the rod-airfoil configuration was carried out in the high-speed subsonic anechoic wind tunnel [1] of the Ecole Centrale de Lyon. A symmetric NACA0012 airfoil (chord $c = 0.1$ m) and a circular rod ($d/c = 0.1$) were placed in the potential core of a jet. The airfoil was located one chord-length downstream of the rod. Both bodies extended $30d$ in the spanwise direction and were supported by rigid smooth plates. The incoming velocity was 72 m/s with a turbulence intensity $Tu = 0.8\%$. The corresponding rod diameter based Reynolds number Re_d was about 48000 , that of the chord length was 480000 and the Mach number M is approximately 0.2 .

3.2. Numerical setup and grids

The computational grids for the flow simulations are of the same dimension and are depicted in Figure 1. The detailed parameters are given in Table 1. Both grids for DES and iLES using 30 cells in the spanwise direction with a spacing of $\Delta z = 0.1d$. The mesh resolution in the

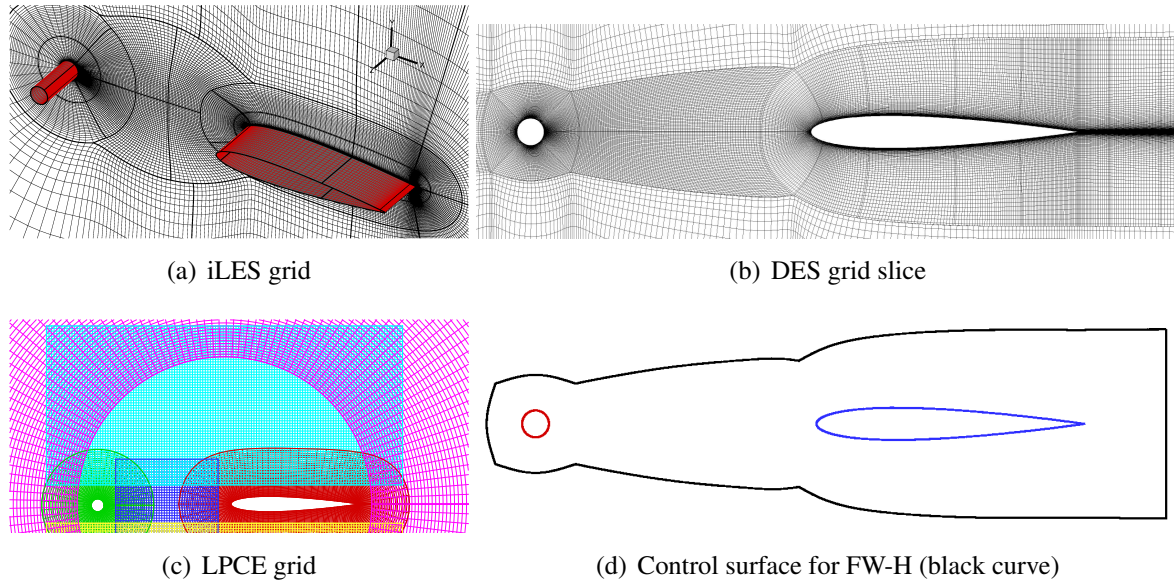


Figure 1. Grids of iLES/LPCE and DES/FW-H

most important area between rod and airfoil is similar for both simulations. The DES uses a fine near wall mesh and grid coarsening in the external blocks, that results in 2.3 million cells. Non-reflecting boundary conditions from Bogey & Bailly [16] are imposed on the farfield boundaries. The time step used in the aerodynamic simulation is 10^{-6} . The integration surface of the FW-H is shown in 1(d). A detailed review of the placement of the integration surface and the influence of volume sources is given by Greschner *et al.* [17]. The near wall mesh of the iLES is rather large, however the gridding rules for an LES leads to a grid of approximately 3.1 million cells. Both simulations using adiabatic no-slip conditions on the solid boundaries and periodic conditions in the spanwise direction. The time step used for iLES and LPCE is $1.833 \cdot 10^{-6}$.

Table 1. Grid parameter for DES, iLES and LPCE

	No. of cells $\cdot 10^6$	Dimension in x	Dimension in y	Dimension in z	Maximum y^+
DES	2.3	$180d$	$120d$	$3d$	1.5
iLES	3.14	$240d$	$240d$	$3d$	12.5
LPCE	0.16	$120d$	$120d$	-	-

The LPCE acoustic grid consists of 0.16 million cells in 6 blocks. It is an overlaid grid which makes it very easy to fit perfectly to the body contour. The grid in the wake region and around the bodies is coarser than the hydrodynamic grid, because the aeroacoustic and hydrodynamic calculation use the same time step and the acoustic information propagates with the speed of sound while the flow propagates roughly with u_∞ . The outer grid size has been chosen in order to resolve the wavelength of an acoustic wave with 10 kHz with 7 cells.

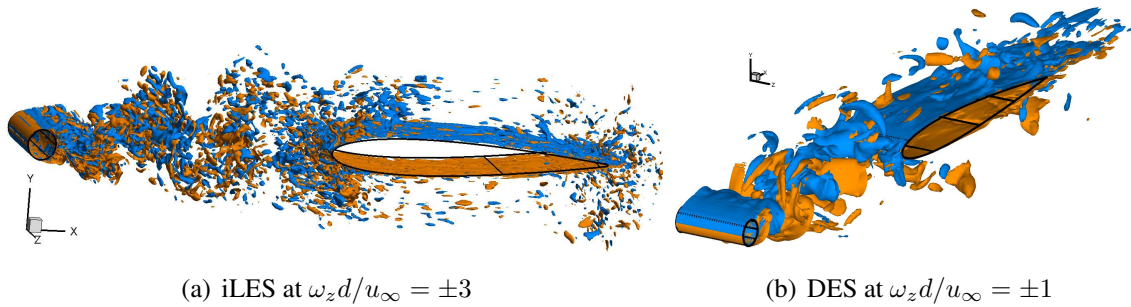


Figure 2. Instantaneous vorticity isosurfaces

4. AERODYNAMICS

The fully three dimensional vortical flows computed with iLES and CEASM DES are shown in Figure 2. In both cases, a vortex shedding pattern can be observed downstream the rod, although strong spanwise effects prevent the formation of a regular Karman vortex street. The non-dimensional shedding frequency is $St \approx 0.183$ for CEASM DES and $St \approx 0.185$ for iLES, and is very close to experimental value of 0.19. The iLES additionally shows small turbulent eddies affecting the large scale structures. This indicates that the iLES calculation clearly benefits from the use of higher order spatial and time discretization schemes and the neglected subgrid-scale model. Figure 3 shows the mean- and rms-velocity profiles in the mid-span plane at different cross-sections sketched on the top plot. The statistics based on approximately 50 shedding cycles. Both, iLES (blue) and CEASM DES (black) show a very similar result for all cross-sections for the mean and fluctuating velocities and are very close to the Hot Wire measurements (red). One exception is the near wake of the rod at position $x/d = -8.7$. On the one hand the fluctuations are overpredicted, Figure 3(c), while on the other hand the velocity wake is too deep. This indicates a too large separation area in the simulations. In Figure 3(d), the results in the front of the airfoil match very well in terms of fluctuations and velocity deficits. In the experiment a slightly asymmetric behaviour in the mean velocity can be recognized, caused by a setup problem in the experiment. The flow a quarter chord length behind the leading edge is depicted in Figure 3(e). The fluctuations agree quite well, but the simulations show a constant offset in the mean velocity. One possible explanation is the test facility, an open jet wind tunnel. The mean velocity of a jet decreases with x , whereas in the simulations a perfect uniform mean flow is given in the whole setup.

The comparison of velocity and fluctuations clarifies that both simulations captured the main physics of the flow. A more detailed investigation of the fluctuations follows by applying a spectral analysis of the flow field. In Figure 4 are shown the velocity spectra S_{uu} at certain locations. Again the experiment is represented by the red line, whereas iLES by the blue and CEASM DES by the black line. The results for the simulations based on spanwise-averaged spectra for DES and time averaged spectra at the mid-span position for iLES. Every figure shows a peak at $St = 0.19$ which indicates that the fluctuations are mainly due to the vortex shedding. The CEASM DES is in a very good agreement in the whole frequency spectra for all depicted locations. The slope of the spectra at higher frequencies including the levels of second harmonic is identical with the experiment. The iLES shows a similar result but overpredicts the levels at frequencies above approximately 3 kHz. This may be due to the neglect of subgrid-scale model in iLES - the small eddies only dissipated by numerical schemes. Both simulations

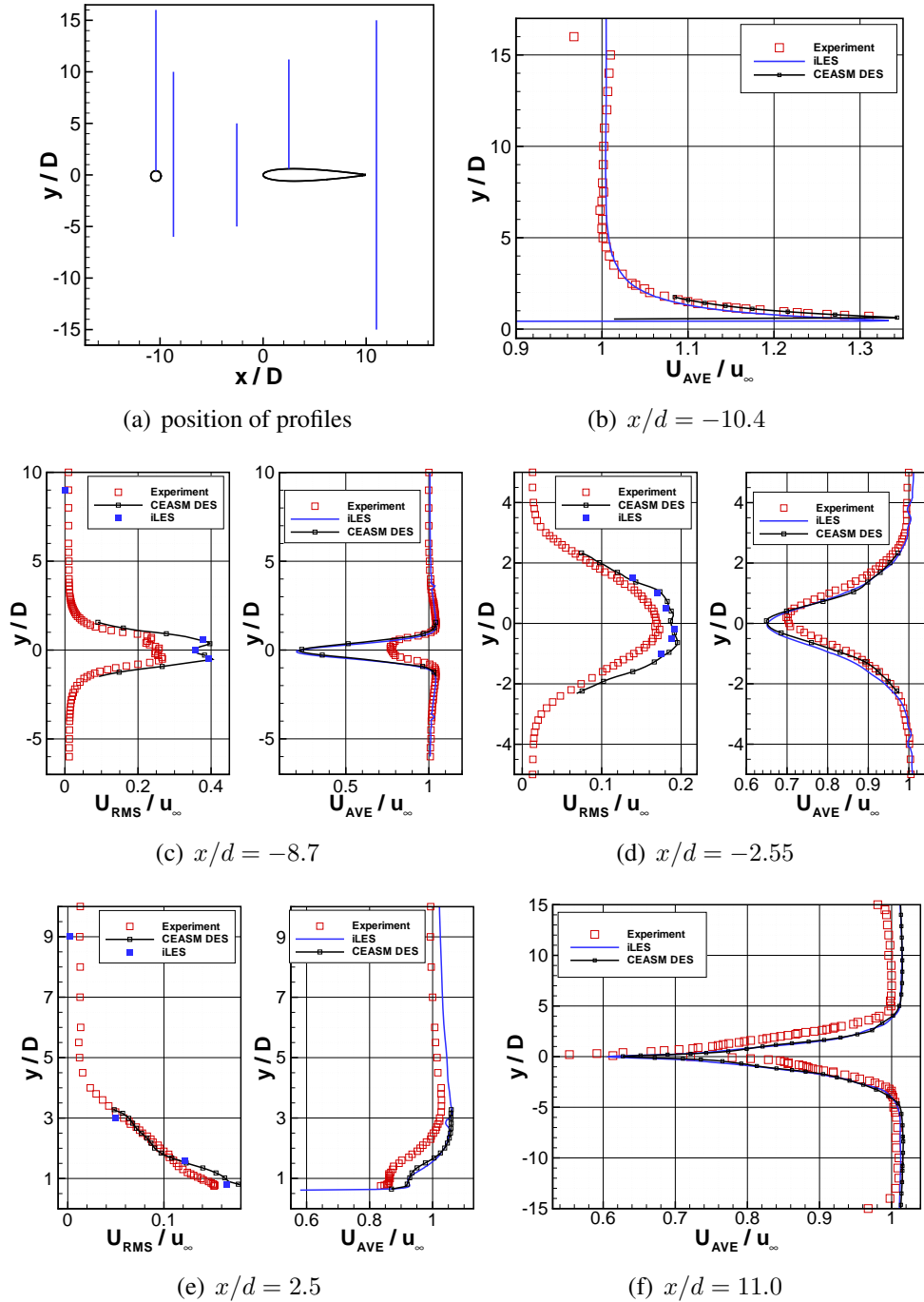
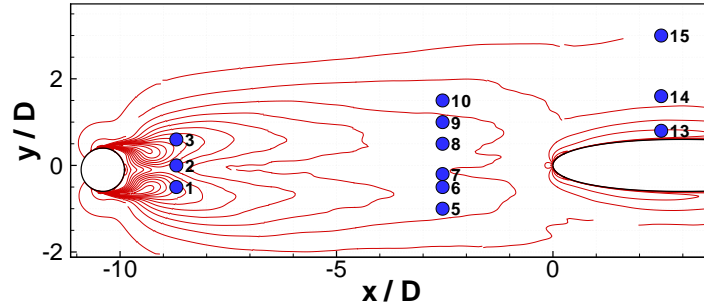


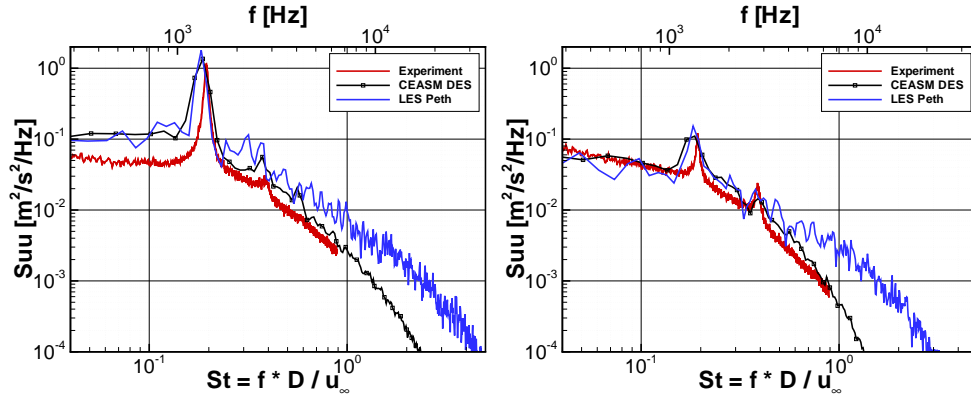
Figure 3. Comparison of mean velocity and RMS value of velocity fluctuations to Hot Wire Anemometry measurements from Jacob *et al.* [1]

show only for position 3 in Figure 4(b), located in the upper shear layer of the rod, overpredicted levels at the very low frequency range.

It can be noted the overall performance of both iLES and CEASM DES is quite impressive and indicates very good results for the aeroacoustic part.

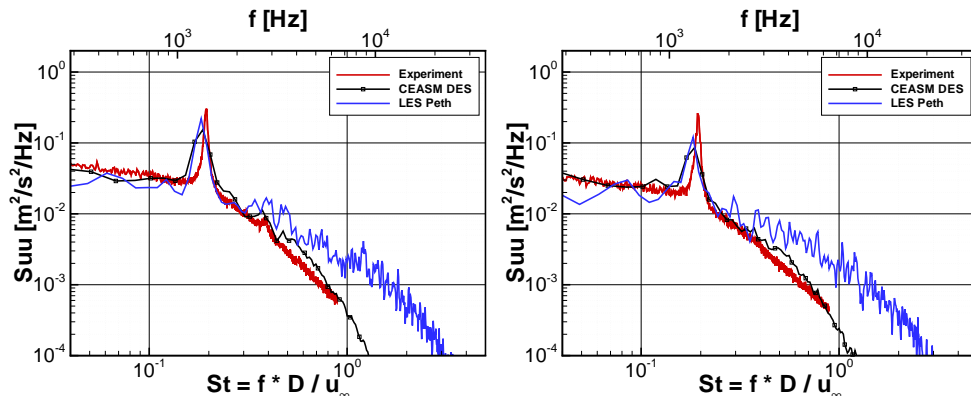


(a) Location of analysis of U_{RMS} with isolines



(b) position 3

(c) position 8



(d) position 9

(e) position 10

Figure 4. Velocity Spectra S_{uu} versus Strouhal number St at different positions compared to Hot Wire Anemometry measurements from Jacob et al. [1]

5. AEROACOUSTICS

The farfield noise is calculated with LPCE and FW-H method based on the unsteady iLES and CEASM DES data, respectively. The observers are located $185d$ from the airfoil midpoint and to the airfoil chord in the midspan plane. The definition of the angle is given in Figure 5(a). The results for 45° , 60° , 90° , 120° and 135° are depicted in Figure 5(b-f). Whereas the experimental data was obtained with a spectral resolution of 4 Hz with 200 averagings, the analysis of the simulated time series leads to a spectral resolutions of 61 Hz and 43 Hz with 6 averaging for DES/FW-H and iLES/LPCE, respectively. All results are expressed in terms of Power Spectral Density (PSD).

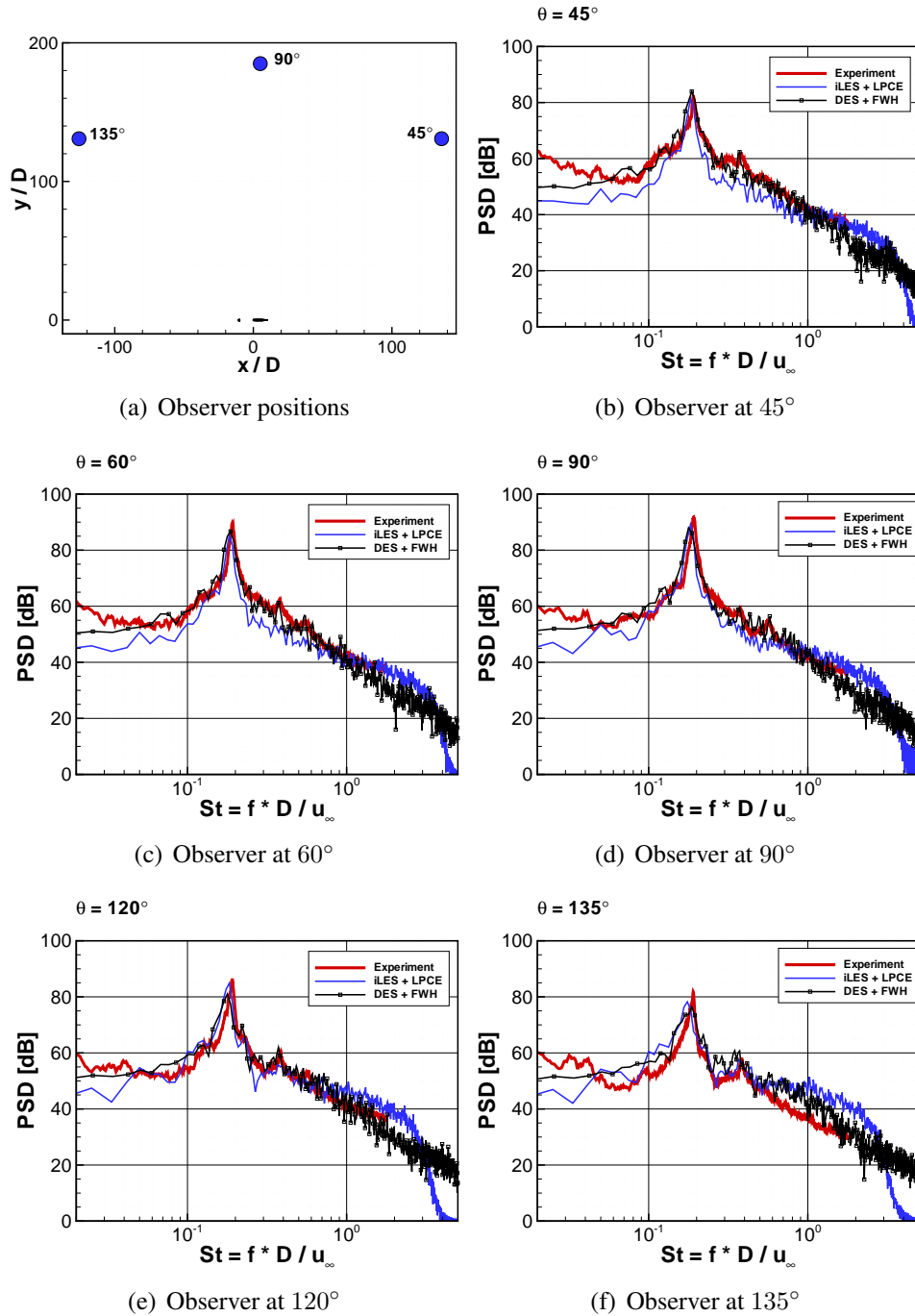


Figure 5. Farfield acoustic PSD compared to measurements from Jacob et al. [1] ($R = 1.85$ m)

The simulated span of three diameters ($L_S = 3d$) is less than the span of the test configuration ($L_{exp} = 30d$), therefore a scaling correction has been applied, as suggested by Kato [18]. The sound pressure level (SPL) of a long span body raises by doubling the dimension in spanwise direction with 3 dB for uncorrelated sources and 6 dB for correlated sources. A new version (combining the three formulas of Kato) of this correction formula between the acoustic

pressure of long span \hat{p}'_L to simulated span \hat{p}'_S is given here [19]

$$|\hat{p}'_L|^2 = |\hat{p}'_S|^2 \underbrace{\sum_{i=1}^N \sum_{j=1}^N \exp \left[-(i-j)^2 \left(\frac{L_S}{L_C} \right)^2 \right]}_{\gamma_N}, \quad \Delta z_{ij} = |z_i - z_j| = |i - j|L_S. \quad (7)$$

Here $L_C(f)$ is the coherence length, L_S the simulated span and N is the number of subsections which each the span of L_S , i.e $L = N \cdot L_S$. The coherence length reaches the maximum of $L_C/d \approx 10$ only in a small bandwidth around the Strouhalpeak and is smaller than one for the whole frequency range at the leading edge of the airfoil ($x/c = 0.02$). This results in a level correction of $\Delta PSD \approx 16.5$ dB around the Strouhal peak and $\Delta PSD = 10$ dB in the rest of the spectra. This correction is used for both simulations. The iLES and the DES predict the peak of the shedding frequency accurately. Its frequency is slightly too small, and the magnitude is underpredicted by 1 to 5 dB for all angles from both methods. The whole broadband spectra of the DES/FW-H shows an excellent agreement with the experiment. The far-field sound predicted by iLES/LPCE is also quite closely compared with the experiment but shows slightly different decaying slopes in the spectra. This is mainly by neglection of the subgrid-scale model in iLES computation.

6. CONCLUSIONS

The overall performance of the presented hybrid methods have proven to be highly satisfactory in the prediction of broadband noise spectrum generated by a complex flow configuration. Both offer a realistic flow picture as shown in section 4 by flow statistics and spectral analysis of velocity. The results of CEASM DES/FW-H method shows clearly the capabilities in simulating the broadband noise sources with advanced hybrid RANS/LES approaches. The far-field sound predicted by iLES/LPCE is also closely compared with the experiment but shows slightly different decaying slopes in the spectra due to the neglection of the subgrid-scale model in iLES. The iLES/LPCE method shows a great potential for broadband turbulent flow noise prediction at low Mach numbers, because reflection, diffraction, and scattering effects of acoustic waves in complex geometries can be included by directly simulating the generation and propagation of the acoustic field. The use of an optimized incompressible LES code for simulating the broadband noise sources with higher order schemes allows to use forcing techniques at boundaries or in the field, without generating spurious noise. Additionally, the approach is not restricted to the 2D wave propagation and therefore applicable to more complicated 3D configurations.

7. ACKNOWLEDGEMENT

The present Korea-German research work was partly supported by the group "Noise generation in turbulent flows" from DFG/CNRS and by the EC founded project "PROBAND".

REFERENCES

- [1] M. C. Jacob, J. Boudet, D. Casalino, M. Michard , “A rod-airfoil experiment as benchmark for broadband noise modeling”, *Journal Theor. Comp. Fluid Dynamics* **19(3)**, (2005).
- [2] B. Greschner, F. Thiele, D. Casalino, M.C. Jacob, “ Influence of turbulence modeling on the broadband noise simulation for complex flows ”, *10th AIAA/CEAS Aeroacoustic Conference, AIAA-2004-2902*, Manchester, UK, (2004).
- [3] J.H. Seo, Y.J. Moon , “Linearized Perturbed Compressible Equations for Low Mach Number Aeroacoustics”, *Journal of Computational Physics, Vol. 218*, pp. 702-719, (2006).
- [4] A.A. Oberai, F. Roknaldin, T.J.R. Hughes, “Trailing Edge Noise due to Turbulent Flows”, *Technical Report No. 02-002*, Boston University, (2002).
- [5] J.E. Ffowcs-Williams, D.L. Hawkings, “Sound generated by turbulence and surfaces in arbitrary motion”, *Phil. trans. Roy. Soc., Series A*, Vol. A264, No. 1151, pp. 321-342, (1969).
- [6] J.H. Ferziger, M. Peric, “Computational Methods for Fluid Dynamics”, *3rd rev. ed. Springer*, ISBN 3-540-42074-6, (2002).
- [7] P.R. Spalart, W.H. Jou, M. Strelets, S.R. Allmaras, “Comments on the feasibility of LES for wings on a hybrid RANS/LES approach”, *Proceedings of 1st AFOSR International Conference on DNS/LES*, pp. 137-147, (1997).
- [8] H. Lübecke, T. Rung, F. Thiele, “Prediction of Spreading Mechanism of 3D Turbulent Wall Jets with Explicit Reynolds-Stress Closures”, *In Engineering Turbulence Modelling and Experiments 5*, pp. 127-145, (2002).
- [9] K.S. Brentner, “A new algorithm for computing acoustic integrals”, *14th IMACS World Congress*, July, (1994).
- [10] F. Farassat, G.P. Succi, “The Prediction of Helicopter Discrete Frequency Noise”, *Vertica*, Vol. 7, No. 4, pp. 309-320, (1983).
- [11] P. Di Francescantonio, “A new boundary integral formulation for the prediction of sound radiation”, *J. Sound and Vibration*, Vol. 202, No. 4, pp. 491-509, (2002).
- [12] K.S. Brentner, F. Farassat, “Analytical Comparison of the Acoustic Analogy and Kirchhof Formulation for Moving Surfaces”, *AIAA Journal*, Vol. 36, No. 8, pp. 1379-1386, (1998).
- [13] D. Casalino, “An advanced time approach for acoustic analogy predictions”, *J. Sound and Vibration*, Vol. 261, No. 4, (2003).
- [14] S.K. Lele, “Compact Finite Difference Schemes with Spectral-like Resolution”, *J. of Computational Physics*, Vol. 103, pp. 16-42, (1992).
- [15] D. Gaitonde, J.S. Shang, J.L. Young, “Practical Aspects of Highorder Accurate Finite-Volume Schemes for Wave Propagation Phenomena”, *International Journal for Numerical Methods in Engineering*, Vol. 45, No. 12, pp. 1849-1869, (1999).
- [16] C. Bogey, C. Bailly, “Three-dimensional non-reflective boundary conditions for acoustic simulations: farfield formulation and validation testcases ”, *Acta Acoustica*, Vol. 88, pp. 463-471, (2002).
- [17] B. Greschner, F. Thiele, D. Casalino, M.C. Jacob, “ Prediction of sound generated by a rod-airfoil configuration using EASM DES and the generalised Lighthill/FW-H analogy”, *Computer and Fluids*, For publication.
- [18] C. Kato, A. Iida, Y. Takano, H. Fujita, M. Ikegawa , “Numerical prediction of aerodynamic noise radiated from low mach turbulent wake ”, *31st Aerospace Sciences Meeting and Exhibit*, (1993).
- [19] J.H.Seo, K.W.Chang, and Y.J.Moon, “Aerodynamic noise prediction for long-span bodies”, *AIAA-Paper 2006-2573*, (2006).